THE GERONTOLOGICAL SOCIETY OF AMERICA®

Journals of Gerontology: Biological Sciences
cite as: *J Gerontol A Biol Sci Med Sci*, 2019, Vol. 74, No. 4, 455–461
doi:10.1093/gerona/gly139
Advance Access publication June 18, 2018

OXFORD

Original Article

Echocardiographic Strain Analysis for the Early Detection of Left Ventricular Systolic/Diastolic Dysfunction and Dyssynchrony in a Mouse Model of Physiological Aging

Claudio de Lucia, MD, PhD,[1,*] Markus Wallner, MD, PhD,[2,3,*] Deborah M. Eaton, MS,[2] Huaqing Zhao, PhD,[4] Steven R. Houser, PhD,[2] and Walter J. Koch, PhD[1]

[1]Center for Translational Medicine and Department of Pharmacology, Lewis Katz School of Medicine, Temple University, Philadelphia, Pennsylvania. [2]Cardiovascular Research Center and Department of Physiology, Lewis Katz School of Medicine, Temple University, Philadelphia, Pennsylvania. [3]Division of Cardiology, Department of Internal Medicine, Medical University of Graz, Graz, Austria. [4]Department of Clinical Sciences, Lewis Katz School of Medicine, Temple University, Philadelphia, Pennsylvania

*Drs. de Lucia and Wallner equally contributed to this article.

Address correspondence to: Walter J. Koch, PhD, Center for Translational Medicine, Lewis Katz School of Medicine, Temple University, 3500 N. Broad Street, 940-MERB, Philadelphia, PA-19140, E-mail: walter.koch@temple.edu

Received: March 7, 2018; Editorial Decision Date: June 12, 2018

Decision editor: Rozalyn M. Anderson, PhD

Abstract

Heart disease is the leading cause of hospitalization and death worldwide, severely affecting health care costs. Aging is a significant risk factor for heart disease, and the senescent heart is characterized by structural and functional changes including diastolic and systolic dysfunction as well as left ventricular (LV) dyssynchrony. Speckle tracking–based strain echocardiography (STE) has been shown as a noninvasive, reproducible, and highly sensitive methodology to evaluate LV function in both animal models and humans. Herein, we describe the efficiency of this technique as a comprehensive and sensitive method for the detection of age-related cardiac dysfunction in mice. Compared with conventional echocardiographic measurements, radial and longitudinal strain, and reverse longitudinal strain were able to detect subtle changes in systolic and diastolic cardiac function in mice at an earlier time point during aging. Additionally, the data show a gradual and consistent decrease with age in regional contractility throughout the entire LV, in both radial and longitudinal axes. Furthermore, we observed that LV segmental dyssynchrony in longitudinal axis reliably differentiated between aged and young mice. Therefore, we propose the use of echocardiographic strain as a highly sensitive and accurate technology enabling and evaluating the effect of new treatments to fight age-induced cardiac disease.

Keywords: Cardiovascular, Animal model, Mice, Senescence, Speckle-tracking echocardiography

The elderly population is rapidly growing worldwide. In the United States and western countries, this phenomenon is the result of both an increase in the birth rate post World War II (Baby Boomer generation) and the drastically longer life expectancies currently seen in the population (1,2). As a result, there will be a doubling of the older population (≥65 years) from the years 2010 to 2040, with the number of elderly people increasing from 40 million in 2010 to 81 million in 2040 (1). An increase in the life expectancy of the population will have a progressively large impact on health care costs for chronic diseases, including cardiovascular diseases. In fact, despite the improvements in diagnosis and treatment, elderly patients still suffer from cardiac diseases such as coronary artery disease, chronic heart failure, arrhythmias, diabetic cardiomyopathy, and hypertensive heart disease (3), showing how age itself is a significant and critical cardiovascular disease risk factor.

The senescent heart is characterized by structural and functional changes including diastolic and systolic dysfunction, left ventricular (LV) hypertrophy, increased fibrotic remodeling, reduced inotropic reserve, and diminished exercise capacity (4–7). These modifications lead to a gradual decline in function and make the aging heart more susceptible to stress and cardiac disease. Therefore, there is an urgent need to identify structural and functional deficiencies in the aged heart before

they become symptomatic and also develop new therapies to counteract or at least delay cardiac aging. The murine model of physiological cardiac aging shows structural and functional changes that are similar to those observed in the human heart (6). Accordingly, the aged mouse has become a valuable tool in understanding the molecular processes modulating aging, as well as identifying novel therapeutic targets (8,9).

Echocardiography (ECHO) has been used in basic and translational research for several years to study models of heart disease, including age-related cardiac dysfunction (9–11). In the last decade, speckle tracking–based echocardiography (STE) has emerged as an interesting and promising tool for the evaluation of myocardial function and dyssynchrony both in humans and animal models, moving beyond the standard echocardiographic measurements (12–20). Few studies have evaluated STE in cardiac aging and have only focused on circumferential strain and suggesting its advantages over standard ECHO. However, the real potential of STE for the evaluation of senescence-induced cardiac dysfunction warrants further investigation (21,22).

In this study, we propose STE as an efficient and noninvasive methodology for the evaluation of LV systolic and diastolic function as well as dyssynchrony in a mouse model of physiological aging. In fact, STE is able to identify subtle changes in LV global/regional strain, relaxation, and synchronicity during aging at earlier stages compared with conventional ECHO.

Methods

Experimental Animals

All animal procedures were performed in accordance with the guidelines of the Institutional Animal Care and Use Committee of Temple University School of Medicine. Forty-three C57BL/6 male mice were studied longitudinally for 20 months. ECHO was performed at 6-, 12-, 15-, and 20-month age. During the study, four mice reached humane endpoints and had to be euthanized, which included three mice before the 15-month time point and one mouse before the 20-month time point.

Conventional ECHO

To assess cardiac structure and function, transthoracic ECHO was performed using a VisualSonics Vevo 2100 system (VisualSonics, Toronto, ON) with a MS400 (30-MHz centerline frequency) probe, as previously described (19,23). In brief, mice were anesthetized with isoflurane (Zoetis IsoFlo, Kalamazoo, MI; induction 3.0% and maintenance 1–3%) and hair was removed from the chest (from the neckline to mid-chest level). Then, mice were placed in a supine position on a heated table (core temperature was maintained at 37°C) with embedded ECG leads. Anesthesia was maintained with 1%–3% isoflurane throughout the procedure.

B- and M-mode images were acquired from a parasternal short-axis view to evaluate LV end-diastolic diameter (LVEDD), end-systolic diameter (LVESD), end-diastolic (LVAW;d) and end-systolic (LVAW;s) anterior wall thickness, end-diastolic (LVPW;d) and end-systolic (LVPW;s) posterior wall thickness, LV mass (LV Mass AW; $1.053 \times ((\text{LVID;d} + \text{LVPW;d} + \text{IVS;d})^3 - \text{LVID;d}^3)$), fractional shortening (FS), and ejection fraction (EF).

Diastolic function was evaluated using conventional ECHO coupled with tissue Doppler and pulsed wave Doppler techniques. From an apical long-axis view, transmitral inflow velocities were recorded by setting the sample volume in the mitral orifice close to the tip of the mitral leaflets. From the pulsed wave Doppler spectral waveforms, we measured the peak early- and late-diastolic transmitral velocities (E and A waves) to obtain the E/A ratio; E-wave deceleration time and isovolumetric relaxation time (IVRT). From the tissue Doppler spectral waveforms, we measured E′ (early-diastolic myocardial relaxation velocity) and calculated E/E′ ratio.

Echocardiographic Speckle Tracking–Based Strain Imaging

STE analyses were performed on parasternal long-axis B-mode loops using a VisualSonics Vevo 2100 system (VisualSonics), as previously described (12,13,19,24–26). Image depth, width, and gain settings were optimized to improve image quality. B-mode loops with a frame rate ≥200 frame/second were utilized for STE. All images were digitally stored in cine loops consisting of 300 frames. All images were acquired and then analyzed using the Vevo Strain Software (Vevo LAB 1.7.1) under their coded numbers in a blinded fashion, then the code was broken, and statistical analysis was performed. Strain, which evaluates changes in length relative to the initial length (strain = final length [L]/initial length [L0]), was calculated either in the radial axis (from the center of the ventricle cavity outward) or longitudinal axis (from the apex to the base; Figure 2A). The strain rate (SR), which is the rate of change of this deformation over time (SR = strain/time), was also measured. Global (calculated with Vevo Strain Software and referred to as global in the text and figures) and regional (six segments: basal, mid, and apical anterior; basal, mid, and apical posterior) LV endocardial longitudinal and radial strain (peak strain %), as well as SR were evaluated (Figure 2B). Regional LV endocardial longitudinal and radial strain/SR were reported as apical versus mid versus basal segments and as anterior (average of basal, mid, and apical) versus posterior (average of basal, mid, and apical). Parasternal long-axis B-mode videos showing vector diagrams for direction and magnitude of endocardial deformation were recorded. EF_{Strain}, cardiac output, and three-dimensional regional endocardial radial strain images (over six LV segments) of four consecutive cardiac cycles (Figure 2D and E) were obtained with Vevo Strain Software.

To measure longitudinal and radial strain/SR during early LV filling, the "reverse peak" algorithm of the Vevo Strain Software was utilized (14). We reported these parameters as reverse radial/longitudinal strain/SR.

LV dyssynchrony was determined from longitudinal strain using three different methods: (a) maximum time-to-peak (T2P) delay between the earliest and the latest segment, (b) time-to-peak variation, defined as the standard deviation (STD) of T2P over all six segments, (c) STD of [T2P/RR interval] for each segment (13,15,25). Of note, RR interval was obtained with Vevo Strain Software. Echocardiographic images of poor quality were excluded from analyses.

Statistical Analysis

For echocardiographic parameters with repeated measures, linear mixed-effects models were used to determine predicted mean values at each assessment point (6, 12, 15, and 20 months) and to test group differences. In each linear mixed-effects model, time was included as fixed effects. Statistical analyses were performed using SAS 9.4 (SAS Institute, Cary, NC). A p value of ≤.05 was used to determine significance for all statistical tests.

Results

Echocardiographic Evaluation of LV Systolic Function

To assess LV changes in systolic function during aging, mice were studied using conventional ECHO and STE at 6-, 12-, 15-, and 20-month

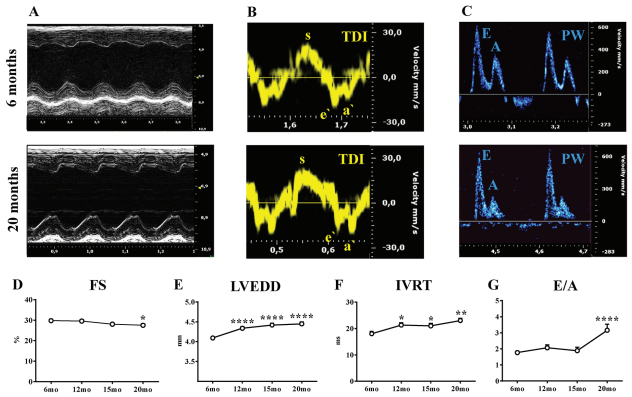

Figure 1. Evaluation of left ventricular systolic and diastolic function with conventional echocardiography. Echocardiographic assessments were performed in each animal at 6-, 12-, 15-, and 20-month age. (**A–C**) representative echo tracings from young (6-month-old, upper panels) and old (20-month-old, lower panel) mice. (A) Representative parasternal short-axis M-mode echocardiograms. (B–C) Diastolic function was determined using echocardiography coupled with tissue Doppler (TDI) (B) and pulsed wave Doppler (PW) (C) techniques. Fractional shortening (FS) (**D**), left ventricular end-diastolic diameter (LVEDD) (**E**), isovolumetric relaxation time (IVRT) (**F**) and E/A ratio (**G**) were measured. n = 15 to 43 mice per group. Data are presented as mean ± SEM. Note: SEM is not shown on the graph if the error bar is shorter than the size of the symbol. *p <.05 versus 6 months, **p <.01 versus 6 months, ****p <.0001 versus 6 months. Linear mixed-effects models were used to test group differences versus 6-month time point.

age. Figure 1A shows representative M-mode images obtained from parasternal short-axis view in young (6-month-old) and aged (20-month-old) mice. Global LV systolic function, reflected by EF and FS, was reduced in aged mice (20-month-old) when compared with young mice (6-month-old; p < .05; Figure 1D and Supplementary Table 1). No differences were found between 12- and 20-month-old mice, and 6-month-old mice. LV end-diastolic diameter, LV end-systolic diameter, and LV Mass AW significantly increased over time, indicating LV remodeling and hypertrophy (6-months vs other time points, p < .0001; Figure 1E and Supplementary Table 1). Next, advanced measures of cardiac contractility such as EF_{Strain}, radial and longitudinal myocardial strain, and SR were performed using parasternal long-axis views. A significant decline in EF_{Strain} was already observed at 12 months, which was 8 months earlier when compared with conventional EF and FS derived from short-axis images (Figure 2C and Supplementary Table 1). Consistent with this finding, radial and longitudinal strain deteriorated over time, starting at as early as 12 months and further declining throughout the rest of the study (Figure 2H and K and Supplementary Table 1). Representative three-dimensional radial strain diagrams, and radial and longitudinal curves from young (6-month-old) and old (20-month-old) mice are shown in Figure 2D–G. Videos of two-dimensional parasternal long-axis loops with vector diagrams, showing direction and magnitude of endocardial deformation, clearly demonstrate differences between young (6-month-old) (Supplementary Video 1) and old (20-month-old) mice (Supplementary Video 2). Radial and longitudinal SR consistently decreased gradually with aging and were reduced in old mice compared with young mice (respectively p < .0001 and p < 1; Supplementary Figure 1A and B, and Supplementary Table 1). STE allows for further quantification of regional LV function. Interestingly, myocardial performance gradually and uniformly decreased in all LV segments starting from 12-month age in mice (Figure 2I, J, L, and M). Radial and longitudinal strains were significantly impaired in old mice compared with young mice in apical,

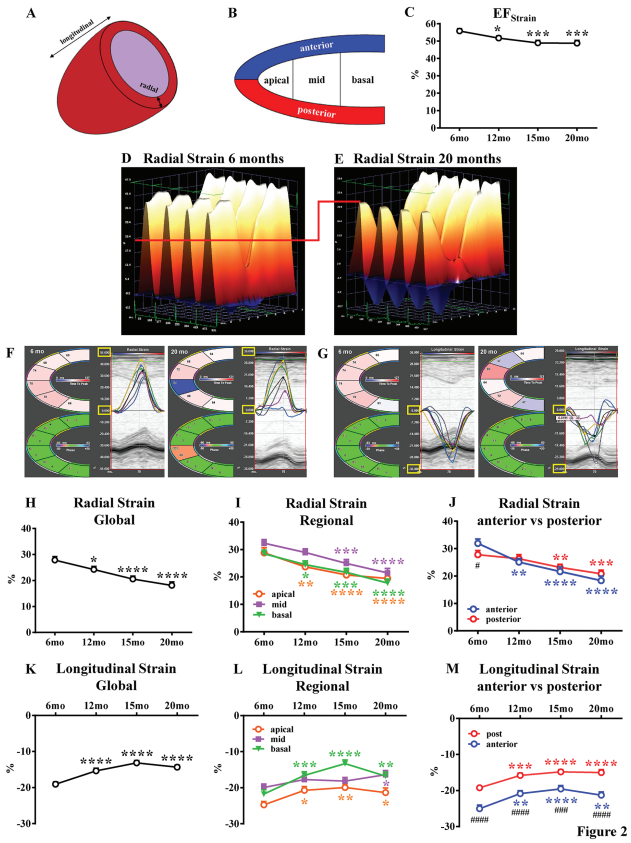

Figure 2. Evaluation of left ventricular systolic function with speckle tracking–based strain echocardiography. Echocardiographic assessments were performed in each animal at 6-, 12-, 15-, and 20-month age. Left ventricular (LV) function involves myocardial deformation along the radial and longitudinal axes: representative picture in (**A**). The LV is divided by Vevo Software into six regional segments: representative picture in (**B**). Ejection fraction (EF_{Strain}) as measured by speckle tracking–based strain echocardiography in (**C**). Three-dimensional LV radial strain deformation shows contraction (orange/positive values) or relaxation (blue/negative values) over six LV segments during four consecutive cardiac cycles for young (6-month-old) and old (20-month-old) groups (**D** and **E**, respectively). Note that LV radial strain deformation has a different scale for young and old mice, as preset by the Vevo Software. To facilitate images' interpretation and comparison of two groups, we have added a red line. Representative LV radial (**F**) and longitudinal (**G**) strain curves (six LV segment) and time-to-peak are shown for young and old groups. Note that to facilitate curves interpretation, maximum and minimum radial and longitudinal strain values for young and old mice have been indicated with yellow boxes. Radial (**H**) and longitudinal (**K**) strain global (average of six LV segments) have been measured. Regional (apical, middle, and basal zone) radial (**I**) and longitudinal (**L**) strain have been evaluated. Radial (**J**) and longitudinal (**M**) strain have been estimated for anterior and posterior walls. n = 36 to 43 mice per group. Data are presented as mean ± SEM. Note: SEM is not shown on the graph if the error bar is shorter than the size of the symbol. *p <.05 versus 6 months, **p <.01 versus 6 months, ***p <.001 versus 6-months, ****p <.0001 versus 6 months; $^{\#}p$ <.05 versus posterior, $^{\#\#\#\#}p$ <.0001 versus posterior. Specific colors for the asterisks have been used in each graph. Linear mixed-effects models were used to test group differences versus 6-month time point or posterior wall.

mid, and basal segments (Figure 2I and L). Interestingly, LV deformation of the anterior and posterior walls was consistently reduced with age in both radial and longitudinal axes (Figure 2J and M). Longitudinal strain values in the anterior wall were significantly better compared with the posterior wall, and this pattern was consistent over time (Figure 2M). Furthermore, aging led to a gradual decrease in cardiac output measured by STE (Supplementary Table 1).

Echocardiographic Evaluation of LV Diastolic Function

LV diastolic function during aging was assessed with conventional ECHO and STE in 6-, 12-, 15-, and 20-month-old mice. LV diastolic function was evaluated with standard ECHO using tissue Doppler and pulsed wave Doppler techniques, as shown in Figure 1B and C. IVRT was significantly prolonged, and deceleration time was reduced in old mice compared with young mice ($p < .01$), indicating impaired LV relaxation (Figure 1F and Supplementary Table 2). E/A ratio was significantly increased in old mice compared with young mice, indicative of more advanced stages of diastolic dysfunction (grade III-IV; $p < .0001$) (Figure 1G and Supplementary Table 2) Surprisingly, E/E′ ratio, a surrogate for LV end-diastolic filling pressures, was reduced in aged mice in our model (Supplementary Table 2).

Reverse longitudinal strain, which reflects myocardial deformation in diastole, was progressively decreased over time (Figure 3B and Supplementary Table 2). Old (20-month-old) mice showed overt impairment in reverse longitudinal strain compared with young (6-month-old) mice ($p < .01$) (Figure 3B and Supplementary Table 2). On the contrary, reverse radial strain as well as reverse longitudinal SR and reverse radial SR were unchanged in old compared with young mice (Figure 3A, Supplementary Figure 1C and D, and Supplementary Table 2).

Echocardiographic Evaluation of LV Dyssynchrony

Age-related LV dyssynchrony was assessed with STE in 6-, 12-, 15-, and 20-month-old mice. Aging resulted in significant LV dyssynchrony regardless of the method used for evaluation. Aged mice showed a significant increase in longitudinal strain maximum T2P delay ($p < .01$), STD (T2P; $p < .01$), and STD [T2P/RR] ($p < .05$; Figure 3F–H and Supplementary Table 2). Interestingly, all these parameters showed early age-related changes at 15 months (Figure 3F–H and Supplementary Table 2). Radial strain maximum T2P delay and STD (T2P) did not differ between old and young mice, while STD [T2P/RR] was increased in older animals, suggesting that radial dyssynchrony is less affected by aging (Figure 3C–E and Supplementary Table 2). Radial and longitudinal SR maximum T2P delay, STD (T2P), and STD [T2P/RR] were unchanged in old mice compared with young mice (Supplementary Figure 2).

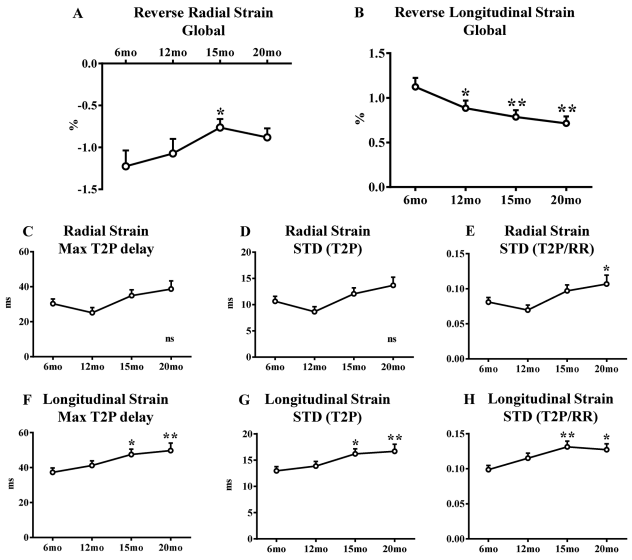

Figure 3: Evaluation of left ventricular diastolic function and dyssynchrony with speckle tracking–based strain echocardiography. Echocardiographic assessments were performed in each animal at 6-, 12-, 15-, and 20-month age. LV diastolic function was assessed: reverse radial (**A**) and longitudinal (**B**) strain global (average of six LV segments) have been measured. LV dyssynchrony has been assessed: radial and longitudinal strain maximum (Max) time-to-peak (T2P) delay (**C** and **F**, respectively), standard deviation (STD) of T2P (**D** and **G**, respectively) and STD of T2P/RR ratio (respectively **E** and **H**) have been measured. $n = 34$ to 43 mice per group. Data are presented as mean ± SEM. Note: SEM is not shown on the graph if the error bar is shorter than the size of the symbol. $^{*}p < .05$ versus 6 month, $^{**}p < .01$ versus 6 months, ns = $p > .05$. Linear mixed-effects models were used to test group differences.

Discussion

Heart disease is the leading cause of hospitalization and death in the United States and western countries (3). Although aging has been underestimated for some time, it is one of the most important risk factors for the development of heart disease, as its incidence and prevalence increase considerably with age (27). Even without the presence of other major risk factors, cardiac aging leads to structural and functional changes. Age-related LV remodeling includes LV hypertrophy and fibrosis; however, the most prominent molecular changes are impaired Ca^{2+} transient/reuptake, β-adrenergic signaling, and mitochondrial dysfunction (6,7,28–30). All these alterations make the heart more vulnerable to several local and systemic stressors (myocardial infarction, hypertension, diabetes, valvulopathies, chemotherapies, etc.) and contribute to increased mortality in the older population. Consequently, there is an unmet need to find novel diagnostic tools and new treatments in order to properly detect and prevent the development of age-related cardiac dysfunction and ultimately improve the quality of life for the elderly.

The purpose of this study was to provide a comparison between conventional echocardiographic measurements and STE analysis to understand whether age-related changes in LV systolic and diastolic function could be detected earlier and more accurately with STE, as previously described in other mouse models and human patients (12,13,20,25,31,32). Furthermore, we assessed whether LV regional contractility and synchronicity were impaired in our mouse model of physiological aging, similar to what has been reported in humans (17). Thus, we followed 43 animals longitudinally for a 20-month period.

We reported that LV FS and EF measured via conventional ECHO were reduced in old mice (20-month-old) compared with young mice (6-month-old); however, these changes are probably nonrelevant from a clinical perspective. Interestingly, most rodent studies report FS and/or EF obtained from parasternal short-axis images, which is not recommended (33). In humans, the EF is calculated based on end-diastolic and end-systolic volumes obtained from apical four-chamber and two-chamber views using the Simpson's biplane method or three-dimensional ECHO. EF has historically been the most important and utilized clinical measure for the evaluation of systolic function (both in patients and animal models of cardiac disease). However, in more recent years, the role of EF has been under evaluation because it is dependent on preload and afterload and is rather a measure of LV remodeling and capacitance than contractility (34,35). Several studies in patients with cardiac disease have shown that despite normal EF, myocardial systolic performance measured by strain was impaired. In fact, STE measurements provide more significant information regarding contractility and have less variability compared with EF (35). For instance, in patients with heart failure with preserved ejection fraction, systolic function was considered to be normal until STE revealed subtle impairments (36).

Therefore, we utilized STE in order to adequately assess myocardial contractility. EF_{Strain} (calculated from a parasternal long-axis view) as well as global radial and longitudinal strain values began deteriorating at 12-month age. Compared with FS or EF derived from conventional short-axis views, STE was able to detect subtle impairments in myocardial contractility at much earlier time points. Moreover, we found that myocardial contractility in apical, mid, and basal segments deteriorated with age to a similar extent, reflected by radial and longitudinal strain values. Interestingly, longitudinal strain values were significantly better in the anterior wall compared with the posterior wall at each time point. Our findings demonstrated the superiority and higher sensitivity of STE in detecting subtle age-dependent changes in LV global and regional systolic function compared with conventional ECHO, as shown in other murine models of cardiac disease (myocardial infarction, pressure overload, chemotherapy-induced cardiotoxicity, and diabetic cardiomyopathy) (12,13,25,26,37,38). Koch colleagues (20) showed that circumferential strain and radial displacement were unchanged during aging in mice. These results are not in line with data from healthy older individuals (impaired longitudinal, radial, and circumferential strain when compared with young and middle-aged adults) and were limited by the retrospective nature of the study, a parasternal short-axis approach, and the evaluation of mice that had not aged enough (16-month-old) (16,21). Derumeaux colleagues instead analyzed only the radial SR in parasternal long axis and interestingly reported that this parameter correlates with the maximal value of the time-varying elastance and end-systolic volume elastance, two well-established load-independent indices of contractility (22). Furthermore, STE allows for early detection of LV dysfunction and predicts clinical outcomes and responses to treatment (eg, cardiac resynchronization therapy) in patients with heart disease (heart failure with preserved ejection fraction, suspected coronary artery disease, and valve disease) (35,36,39,40). Although it is thought that systolic function is usually not impaired during healthy aging, there is now a growing body of evidence that challenges this concept, and therefore, this issue may need to be re-evaluated. In this regard, Crendal colleagues showed that longitudinal strain was impaired in older subjects compared with young healthy subjects, while EF was unaltered (17).

Diastolic function is instead widely recognized to be compromised during aging, especially in the early active relaxation phase (41). Criteria for echocardiographic evaluation of LV diastolic function is well established and validated in humans; however the same methods are controversial when applied to rodent studies due to the animals having high HR and small heart size (14,42). Performing diastolic evaluation can be tricky and multiple echo-derived indices, such as E/A ratio, E/E′ ratio, deceleration time, IVRT, and the left atrial size, should be taken into account (14,42–44). We found that E/A ratio and IVRT significantly increased in aged mice compared with young mice, while deceleration time became shorter. These results are consistent with a restrictive-like phenotype in humans. However, we were not able to consistently measure E/A ratios in all animals due to fusion of E and A waves at a higher HR, as previously described by others (14). These technical difficulties can partially explain the variability in E/A ratio values in aged mice reported by several authors (44,45). The E/E′ ratio was reduced in aged mice compared with young mice, which is different than data collected from elderly patients (43). Koch colleagues instead found that E/E′ ratio was similar in young and aged mice (21). Therefore, the E/E′ ratio is not a reliable parameter for the evaluation of diastolic function during aging in mice, consistent with the findings of a recent report in murine volume overload and heart failure with preserved ejection fraction models (14). Reverse longitudinal SR has been shown to mirror the impairment of LV relaxation in both patients and animal models of diastolic dysfunction (14,46). We found global reverse longitudinal strain to occur early (12 months) and gradually decrease with age. On the contrary, global reverse radial strain was not different between young (6-month-old) and aged (20-month-old) mice. This is an interesting finding because due to variation of myocardial fiber orientation at different levels of the LV wall, longitudinal strain is most representative of myocardial deformation at the level of the endocardium, while radial strain mainly represents mid-myocardial layers (12). Therefore, our data suggest that relaxation is predominantly impaired in subendocardial layers. Furthermore, observed prolongation of IVRT in aged mice indicates that active relaxation (thick–thin filament dissociation, ATP-dependent Ca^{2+} reuptake) in early diastole is impaired, where approximately 80% of LV filling is achieved (47). This finding is consistent with previously reported reductions in sarco/endoplasmic reticulum Ca^{2+}-ATPase activity during normal aging (7).

In recent years, intraventricular dyssynchrony has been shown to be an important prognostic factor in patients with heart disease (48). This parameter, which is quantified with STE, allows for predicting the response to cardiac resynchronization therapy in heart failure patients (40,48). Several mouse models of cardiac dysfunction, such as pressure overload, myocardial infarction, or dilated cardiomyopathy, are associated with a dyssynchronous profile, which interferes with appropriate contractile function (13,15,26). Recent studies using magnetic resonance imaging or longitudinal strain maximum delay have shown that LV dyssynchrony is altered across the lifespan of healthy subjects (17,49,50). In our study, LV dyssynchrony in longitudinal axis reliably differentiated between aged (15- and 20- month-old) and young (6-month-old) mice. This result was confirmed through three different methodologies (see Methods section). Radial strain dyssynchrony was altered in old compared with young mice only in the STD [T2P/RR] formula, suggesting that subendocardial layers are more susceptible to dyssynchrony, which is in line with what we observed in reverse longitudinal strain. Impaired age-related LV mechanical synchronicity can be explained at least in part by increased fibrosis and lipid content in aged hearts (17,51).

Our work is the first to show noninvasive comprehensive profiling of LV contractility, relaxation, and synchronicity in mice during normal aging. STE is highly sensitive and provides insight regarding early changes in LV function during aging, whereas conventional ECHO is unable to detect such subtle changes. Our results in mice are in line with data published by Crendal colleagues, which described an increase in myocardial dysfunction and dyssynchrony (both evaluated with STE) in healthy males throughout their lifespan (17). Our approach may be a useful and accurate methodology to serially monitor the effects on LV function of pharmaceutical drugs, dietary treatments, gene-therapy, gene-editing (eg, via CRISPR-Cas9), or micro RNA–targeting therapies in the murine model of aging (9,27,52,53). This is crucial as the elderly population significantly increases, and we must urgently identify new treatments to counteract or curb senescence-related cardiac dysfunction (1,2,52).

Limitations

STE requires high-quality images at high frame rates (>200/sec). For this purpose, our study utilized a highly qualified and trained echocardiographer for acquiring and analyzing the images. An inherent limitation of software-based analysis is the variation in algorithms between different vendors, which also limits the ability to compare

results derived from different programs (25). Future studies are required to establish complete standardization of strain measurements in animal models of diseases like physiological aging. Another limitation of our study is the lack of a female group. We are aware that gender is an important biological factor in the pathophysiology of the cardiovascular system; however, we did not include female mice in our study as we were focused on the evaluation of the effect of age, rather than sex on cardiac function throughout the lifespan. Anesthetics (isoflurane in our study) can potentially affect cardiac function via direct effects or by reducing the HR because cardiac function in mice is associated with HR. However, several studies have shown that HR in our reported range yields reliable and consistent measurements (25,54). In our study, we observed statistical differences in HR at 12- and 15-month time points compared with 6 months (both in conventional ECHO and STE) but saw no differences between 20-month and 6-month time points. However, higher HRs did not cause an increase in inotropy, and we do not believe that these small differences are of clinical relevance and do not affect our results. In fact, although we observed a slight increase in the HRs of 15- and 20-month-old mice compared with 6-month-old mice, these changes were concomitant with impaired STE parameters rather than an improvement.

Supplementary Material

Supplementary data are available at *The Journals of Gerontology, Series A: Biological Sciences and Medical Sciences* online.

Funding

This work was supported by National Institutes of Health (NIH P01 HL091799, NIH R37 HL061690, NIH P01 HL075443 [Project 2] to W.J.K.; NIH P01 HL091799 [Project 3] to S.R.H.) and American Heart Association (postdoctoral fellowship 17POST33660942 to C.d.L.).

Conflict of interest

The authors declare that the research was conducted in the absence of any commercial or financial relationships that could be construed as a potential conflict of interest.

References

1. Odden MC, Coxson PG, Moran A, Lightwood JM, Goldman L, Bibbins-Domingo K. The impact of the aging population on coronary heart disease in the United States. *Am J Med*. 2011;124:827–833.e5. doi:10.1016/j.amjmed.2011.04.010
2. Centers for Disease Control and Prevention (CDC). Trends in aging—United States and worldwide. *MMWR Morb Mortal Wkly Rep*. 2003;52:101–104, 106.
3. Benjamin EJ, Blaha MJ, Chiuve SE, et al.; American Heart Association Statistics Committee and Stroke Statistics Subcommittee. Heart disease and stroke statistics-2017 update: a report from the American Heart Association. *Circulation*. 2017;135:e146–e603. doi:10.1161/CIR.0000000000000485
4. Nakou ES, Parthenakis FI, Kallergis EM, Marketou ME, Nakos KS, Vardas PE. Healthy aging and myocardium: a complicated process with various effects in cardiac structure and physiology. *Int J Cardiol*. 2016;209:167–175. doi:10.1016/j.ijcard.2016.02.039
5. Scalia GM, Khoo SK, O'Neill S; LAW Study Group. Age-related changes in heart function by serial echocardiography in women aged 40-80 years. *J Womens Health (Larchmt)*. 2010;19:1741–1745. doi:10.1089/jwh.2009.1752
6. Dai DF, Chen T, Johnson SC, Szeto H, Rabinovitch PS. Cardiac aging: from molecular mechanisms to significance in human health and disease. *Antioxid Redox Signal*. 2012;16:1492–1526. doi:10.1089/ars.2011.4179
7. Feridooni HA, Dibb KM, Howlett SE. How cardiomyocyte excitation, calcium release and contraction become altered with age. *J Mol Cell Cardiol*. 2015;83:62–72. doi:10.1016/j.yjmcc.2014.12.004
8. Liao CY, Kennedy BK. Mouse models and aging: longevity and progeria. *Curr Top Dev Biol*. 2014;109:249–285. doi:10.1016/B978-0-12-397920-9.00003-2
9. Tang T, Hammond HK, Firth A, et al. Adenylyl cyclase 6 improves calcium uptake and left ventricular function in aged hearts. *J Am Coll Cardiol*. 2011;57:1846–1855. doi:10.1016/j.jacc.2010.11.052
10. Scherrer-Crosbie M, Kurtz B. Ventricular remodeling and function: insights using murine echocardiography. *J Mol Cell Cardiol*. 2010;48:512–517. doi:10.1016/j.yjmcc.2009.07.004
11. Reddy AK, Amador-Noguez D, Darlington GJ, et al. Cardiac function in young and old Little mice. *J Gerontol A Biol Sci Med Sci*. 2007;62:1319–1325.
12. Bauer M, Cheng S, Jain M, et al. Echocardiographic speckle-tracking based strain imaging for rapid cardiovascular phenotyping in mice. *Circ Res*. 2011;108:908–916. doi:10.1161/CIRCRESAHA.110.239574
13. Bauer M, Cheng S, Unno K, Lin FC, Liao R. Regional cardiac dysfunction and dyssynchrony in a murine model of afterload stress. *PLoS One*. 2013;8:e59915. doi:10.1371/journal.pone.0059915
14. Schnelle M, Catibog N, Zhang M, et al. Echocardiographic evaluation of diastolic function in mouse models of heart disease. *J Mol Cell Cardiol*. 2018;114:20–28. doi:10.1016/j.yjmcc.2017.10.006
15. Yamada S, Arrell DK, Kane GC, et al. Mechanical dyssynchrony precedes QRS widening in ATP-sensitive K^+ channel-deficient dilated cardiomyopathy. *J Am Heart Assoc*. 2013;2:e000410. doi:10.1161/JAHA.113.000410
16. Xia JZ, Xia JY, Li G, Ma WY, Wang QQ. Left ventricular strain examination of different aged adults with 3D speckle tracking echocardiography. *Echocardiography*. 2014;31:335–339. doi:10.1111/echo.12367
17. Crendal E, Dutheil F, Naughton G, McDonald T, Obert P. Increased myocardial dysfunction, dyssynchrony, and epicardial fat across the lifespan in healthy males. *BMC Cardiovasc Disord*. 2014;14:95. doi:10.1186/1471-2261-14-95
18. Ram R, Mickelsen DM, Theodoropoulos C, Blaxall BC. New approaches in small animal echocardiography: imaging the sounds of silence. *Am J Physiol Heart Circ Physiol*. 2011;301:H1765–H1780. doi:10.1152/ajpheart.00559.2011
19. Wallner M, Duran JM, Mohsin S, et al. Acute catecholamine exposure causes reversible myocyte injury without cardiac regeneration. *Circ Res*. 2016;119:865–879. doi:10.1161/CIRCRESAHA.116.308687
20. Zheng M, Pan F, Liu Y, et al. Echocardiographic strain analysis for the early detection of myocardial structural abnormality and initiation of drug therapy in a mouse model of dilated cardiomyopathy. *Ultrasound Med Biol*. 2017;43:2914–2924. doi:10.1016/j.ultrasmedbio.2017.07.020
21. Koch SE, Haworth KJ, Robbins N, et al. Age- and gender-related changes in ventricular performance in wild-type FVB/N mice as evaluated by conventional and vector velocity echocardiography imaging: a retrospective study. *Ultrasound Med Biol*. 2013;39:2034–2043. doi:10.1016/j.ultrasmedbio.2013.04.002
22. Derumeaux G, Ichinose F, Raher MJ, et al. Myocardial alterations in senescent mice and effect of exercise training: a strain rate imaging study. *Circ Cardiovasc Imaging*. 2008;1:227–234. doi:10.1161/CIRCIMAGING.107.745919
23. Benavides-Vallve C, Corbacho D, Iglesias-Garcia O, et al. New strategies for echocardiographic evaluation of left ventricular function in a mouse model of long-term myocardial infarction. *PLoS One*. 2012;7:e41691. doi:10.1371/journal.pone.0041691
24. Duran JM, Makarewich CA, Sharp TE, et al. Bone-derived stem cells repair the heart after myocardial infarction through transdifferentiation and paracrine signaling mechanisms. *Circ Res*. 2013;113:539–552. doi:10.1161/CIRCRESAHA.113.301202
25. Shepherd DL, Nichols CE, Croston TL, et al. Early detection of cardiac dysfunction in the type 1 diabetic heart using speckle-tracking based strain imaging. *J Mol Cell Cardiol*. 2016;90:74–83. doi:10.1016/j.yjmcc.2015.12.001

26. Bhan A, Sirker A, Zhang J, et al. High-frequency speckle tracking echocardiography in the assessment of left ventricular function and remodeling after murine myocardial infarction. *Am J Physiol Heart Circ Physiol*. 2014;306:H1371–H1383. doi:10.1152/ajpheart.00553.2013
27. Chiao YA, Rabinovitch PS. The aging heart. *Cold Spring Harb Perspect Med*. 2015;5:a025148. doi:10.1101/cshperspect.a025148
28. Kong CHT, Bryant SM, Watson JJ, et al. The effects of aging on the regulation of T-tubular ICa by caveolin in mouse ventricular myocytes. *J Gerontol A Biol Sci Med Sci*. 2018;73:711–719. doi:10.1093/gerona/glx242
29. Emelyanova L, Preston C, Gupta A, et al. Effect of aging on mitochondrial energetics in the human atria. *J Gerontol A Biol Sci Med Sci*. 2018;73:608–616. doi:10.1093/gerona/glx160
30. Horn MA, Bode EF, Borland SJ, et al. Temporal development of autonomic dysfunction in heart failure: effects of age in an ovine rapid-pacing model. *J Gerontol A Biol Sci Med Sci*. 2016;71:1544–1552. doi:10.1093/gerona/glv217
31. Murtaza G, Virk HUH, Khalid M, et al. Role of speckle tracking echocardiography in dilated cardiomyopathy: a review. *Cureus*. 2017;9:e1372. doi:10.7759/cureus.1372
32. Tadic M, Pieske-Kraigher E, Cuspidi C, et al. Left ventricular strain and twisting in heart failure with preserved ejection fraction: an updated review. *Heart Fail Rev*. 2017;22:371–379. doi:10.1007/s10741-017-9618-3
33. Chengode S. Left ventricular global systolic function assessment by echocardiography. *Ann Card Anaesth*. 2016;19(suppl 1):S26–S34. doi:10.4103/0971-9784.192617
34. Konstam MA, Abboud FM. Ejection fraction: misunderstood and overrated (changing the paradigm in categorizing heart failure). *Circulation*. 2017;135:717–719. doi:10.1161/CIRCULATIONAHA.116.025795
35. Potter E, Marwick TH. Assessment of left ventricular function by echocardiography: the case for routinely adding global longitudinal strain to ejection fraction. *JACC Cardiovasc Imaging*. 2018;11:260–274. doi:10.1016/j.jcmg.2017.11.017
36. Shah AM, Claggett B, Sweitzer NK, et al. Prognostic importance of impaired systolic function in heart failure with preserved ejection fraction and the impact of spironolactone. *Circulation*. 2015;132:402–414. doi:10.1161/CIRCULATIONAHA.115.015884
37. Rea D, Coppola C, Barbieri A, et al. Strain analysis in the assessment of a mouse model of cardiotoxicity due to chemotherapy: sample for preclinical research. *In Vivo*. 2016;30:279–290.
38. Li RJ, Yang J, Yang Y, et al. Speckle tracking echocardiography in the diagnosis of early left ventricular systolic dysfunction in type II diabetic mice. *BMC Cardiovasc Disord*. 2014;14:141. doi:10.1186/1471-2261-14-141
39. Blessberger H, Binder T. Two dimensional speckle tracking echocardiography: clinical applications. *Heart*. 2010;96:2032–2040. doi:10.1136/hrt.2010.199885
40. Suffoletto MS, Dohi K, Cannesson M, Saba S, Gorcsan J, III. Novel speckle-tracking radial strain from routine black-and-white echocardiographic images to quantify dyssynchrony and predict response to cardiac resynchronization therapy. *Circulation*. 2006;113:960–968. doi:10.1161/CIRCULATIONAHA.105.571455
41. Strait JB, Lakatta EG. Aging-associated cardiovascular changes and their relationship to heart failure. *Heart Fail Clin*. 2012;8:143–164. doi:10.1016/j.hfc.2011.08.011
42. Nagueh SF, Smiseth OA, Appleton CP, et al.; Houston, Texas; Oslo, Norway; Phoenix, Arizona; Nashville, Tennessee; Hamilton, Ontario, Canada; Uppsala, Sweden; Ghent and Liège, Belgium; Cleveland, Ohio; Novara, Italy; Rochester, Minnesota; Bucharest, Romania; and St. Louis, Missouri. Recommendations for the evaluation of left ventricular diastolic function by echocardiography: an update from the American Society of Echocardiography and the European Association of Cardiovascular Imaging. *Eur Heart J Cardiovasc Imaging*. 2016;17:1321–1360. doi:10.1093/ehjci/jew082
43. Dugo C, Rigolli M, Rossi A, Whalley GA. Assessment and impact of diastolic function by echocardiography in elderly patients. *J Geriatr Cardiol*. 2016;13:252–260. doi:10.11909/j.issn.1671-5411.2016.03.008
44. Medrano G, Hermosillo-Rodriguez J, Pham T, et al. Left atrial volume and pulmonary artery diameter are noninvasive measures of age-related diastolic dysfunction in mice. *J Gerontol A Biol Sci Med Sci*. 2016;71:1141–1150. doi:10.1093/gerona/glv143
45. Signore S, Sorrentino A, Borghetti G, et al. Late Na(+) current and protracted electrical recovery are critical determinants of the aging myopathy. *Nat Commun*. 2015;6:8803. doi:10.1038/ncomms9803
46. Choudhury A, Magoon R, Malik V, Kapoor PM, Ramakrishnan S. Studying diastology with speckle tracking echocardiography: the essentials. *Ann Card Anaesth*. 2017;20(suppl 1):S57–S60. doi:10.4103/0971-9784.197800
47. Andersen MJ, Borlaug BA. Invasive hemodynamic characterization of heart failure with preserved ejection fraction. *Heart Fail Clin*. 2014;10:435–444. doi:10.1016/j.hfc.2014.03.001
48. Cai Q, Ahmad M. Left ventricular dyssynchrony by three-dimensional echocardiography: current understanding and potential future clinical applications. *Echocardiography*. 2015;32:1299–1306. doi:10.1111/echo.12965
49. Rosen BD, Fernandes VR, Nasir K, et al. Age, increased left ventricular mass, and lower regional myocardial perfusion are related to greater extent of myocardial dyssynchrony in asymptomatic individuals: the multi-ethnic study of atherosclerosis. *Circulation*. 2009;120:859–866. doi:10.1161/CIRCULATIONAHA.108.787408
50. Föll D, Jung B, Germann E, Hennig J, Bode Ch, Markl M. Magnetic resonance tissue phase mapping: analysis of age-related and pathologically altered left ventricular radial and long-axis dyssynchrony. *J Magn Reson Imaging*. 2011;34:518–525. doi:10.1002/jmri.22641
51. Lin LY, Wu CK, Juang JM, et al. Myocardial regional interstitial fibrosis is associated with left intra-ventricular dyssynchrony in patients with heart failure: a cardiovascular magnetic resonance study. *Sci Rep*. 2016;6:20711. doi:10.1038/srep20711
52. de Lucia C, Komici K, Borghetti G, et al. microRNA in cardiovascular aging and age-related cardiovascular diseases. *Front Med (Lausanne)*. 2017;4:74. doi:10.3389/fmed.2017.00074
53. Cieslik KA, Sekhar RV, Granillo A, et al. Improved cardiovascular function in old mice after n-acetyl cysteine and glycine supplemented diet: inflammation and mitochondrial factors. *J Gerontol A Biol Sci Med Sci*. 2018. doi:10.1093/gerona/gly034
54. Wu J, Bu L, Gong H, et al. Effects of heart rate and anesthetic timing on high-resolution echocardiographic assessment under isoflurane anesthesia in mice. *J Ultrasound Med*. 2010;29:1771–1778. doi:10.7863/jum.2010.29.12.1771